ELSEVIER

Surface Science 334 (1995) L730–L734

surface science

Surface Science Letters

Adsorption properties of porous silicon characterized by optically enhanced ^{129}Xe NMR spectroscopy

T. Pietrass *, A. Bifone, A. Pines

Department of Chemistry, University of California at Berkeley and Lawrence Berkeley Laboratories, Berkeley, CA 94720, USA

Received 30 January 1995; accepted for publication 31 March 1995

Abstract

Highly spin polarized xenon is used to study the adsorption properties of porous silicon surfaces by ^{129}Xe NMR spectroscopy. The sensitivity enhancement through optical pumping allows the NMR characterization of small amounts of physisorbed xenon in a pressure regime typical for adsorption isotherms. Fully hydrogen terminated porous silicon, porous silicon with an increased number of dangling bonds and porous silicon after methanol adsorption are characterized by the adsorbed ^{129}Xe NMR lineshape, chemical shift and relaxation behavior.

Keywords: Nuclear magnetic resonance; Physical adsorption; Surface structure

Since the discovery of the visible luminescence of porous silicon at low temperatures [1] and, more recently, at room temperature [2], various applications of porous silicon have been discussed, mainly as electrooptic [3] devices. The photoluminescence of porous silicon – the origin of which has been subject of much debate [4] – depends on porosity [5] and on surface treatment [6,7] of the sample. The luminescence can be reversibly quenched by adsorbing organic solvent molecules [8]. The reversible quenching phenomenon has been attributed to surface state trapping by alignment of molecular dipoles on the surface, which provides a nonradiative recombination pathway for surface electrons and holes. Molecules which exhibit large dipole moments, such as ethanol and methanol, are most efficient in quenching the luminescence. Emission spectra of porous silicon after exposure to different vapors recovered to the original intensity within seconds [8]. Multiple exposure–evacuation cycles resulted in the same quenching ratios indicating that the surface structure of the porous silicon is not altered upon vapor adsorption [9]. The degree of quenching and the change in the photoluminescence wavelength are determined by the nature of the adsorbate molecule, which suggests the use of porous silicon as a chemical sensor [9,10].

Since the pioneering work of Fraissard and coworkers [11], ^{129}Xe nuclear magnetic resonance (NMR) spectroscopy has been widely applied to probe surfaces and confined spaces [12]. Using xenon as a chemically inert surface probe, we have studied the effect of methanol adsorption on porous silicon. The xenon adsorption properties were characterized by ^{129}Xe NMR spectroscopy and simultaneously in terms of an adsorption isotherm. The ^{129}Xe NMR detection sensitivity was substantially enhanced by optical pumping [13,14].

* Corresponding author.
E-mail: tanya@dirac.cchem.berkeley.edu

0039-6028/95/$09.50 © 1995 Elsevier Science B.V. All rights reserved
SSDI 0039-6028(95)00525-0

SURFACE SCIENCE LETTERS

The sample consisted of ca. 10 mg of free standing porous silicon which had been prepared by anodic etching (current density 30 mA/cm^2) of a B-doped Si substrate with a resistivity of 5 Ω cm^{-1} in a 48% hydrofluoric acid solution. The wafers were etched with the (100) surface exposed. The porous silicon sample was treated in three different ways, each of which provided a different sample for the NMR experiments. The first NMR sample was obtained by etching the original sample again for about 2 min without current in 48% hydrofluoric acid solution to ensure hydrogen termination of the surface [15]; this sample will be referred to as "hydrogen terminated". After the first set of NMR experiments, the xenon was desorbed from the surface by warming the sample to room temperature and evacuating it. Heating this sample under vacuum (10^{-5} Torr) to 400°C for 7 min increased the number of dangling bonds on the surface from 10^{16}/cm^3 to 10^{19}/cm^3 [16] and provided the second NMR sample ("heat treated"). Following the NMR experiments on the heat treated sample, the xenon was desorbed as described above. Then, the sample was exposed to an equilibrium pressure of 100 Torr of degassed methanol vapor at room temperature, which yielded the third sample for the NMR experiments ("methanol covered"). The amount of adsorbed methanol was sufficient to cover completely the surface of the porous silicon.

The optical pumping cell, described in detail elsewhere [14], was located directly beneath the bore of the superconducting magnet. The sample tube in the NMR probe was connected through glassware with the optical pumping cell, a pressure gauge and a vacuum line. The sample was equilibrated to low temperatures by a flow of cold nitrogen gas. The NMR experiments were performed at various temperatures. Chemical shifts for the adsorbed xenon increased with decreasing temperatures, as has been observed previously [14]. Only spectra obtained at 123 K will be discussed. The home-built NMR probe was equipped with a solenoid coil providing a typical duration of 8.35 μs for a 90° pulse at the ^{129}Xe Larmor frequency of 49.45 MHz. Chemical shift values are referenced to xenon gas at low pressures (0 ppm).

After optical polarization [13,14], a small fraction of the xenon was admitted to the sample. Ten seconds later, when the pressure had stabilized, the NMR signal was acquired following a single radiofrequency pulse. Recording the initial and final xenon pressures allowed us to estimate the amount of adsorbed xenon.

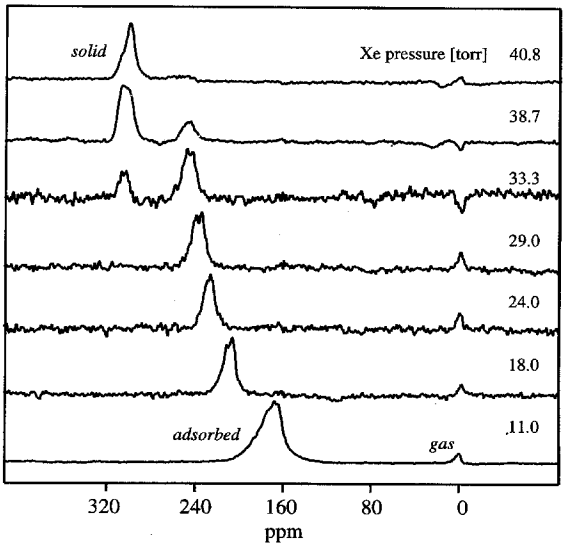

Fig. 1. ^{129}Xe NMR spectra for xenon physisorbed on hydrogen terminated porous silicon for increasing xenon pressures at 123 K. The resonances for gas, solid and physisorbed xenon are indicated. The spectra are scaled to the same maximum amplitude.

In Fig. 1, the pressure dependent ^{129}Xe NMR spectra of xenon adsorbed onto hydrogen terminated porous silicon are displayed. At low pressures a single resonance is observed, which shifts downfield with increasing xenon pressure. At 33 Torr, a second resonance at 310 ppm appears, assigned to solid xenon, and indicating that saturation coverage of the porous silicon surface has been achieved. Any excess xenon added to the system freezes on the walls of the sample tube. With the occurrence of the signal of solid xenon, the resonance of the physisorbed xenon reaches a limiting chemical shift value of 250 ppm. The signal intensity of this peak decreases upon addition of more xenon, since no more fresh xenon is physisorbed and the non-equilibrium polarization is destroyed by applying radiofrequency pulses and by spin lattice relaxation. With increasing pressure, the resonance of the physisorbed xenon narrows. The same effect has been observed on cadmium sulfide nanocrystals and was attributed to an increase in the

SURFACE SCIENCE LETTERS

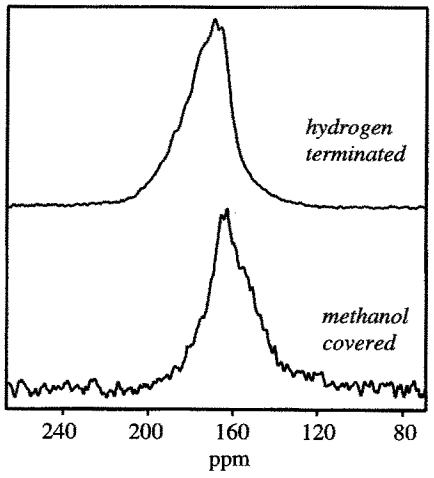

Fig. 2. ^{129}Xe NMR lineshapes for the signals of physisorbed xenon on hydrogen terminated porous silicon (Xe pressure = 11 Torr) and on methanol covered porous silicon (15 Torr).

homogeneity of the xenon environment as the xenon–xenon interactions become more dominant [17]. The lineshape of the xenon frozen on the walls of the sample container has been discussed in Ref. [18] in terms of susceptibility effects. The small resonance at 0 ppm originates from xenon in the gas phase. In the course of the experiment, the phase of the gas peak changes, which is due to the long relaxation time of the xenon gas [19]. A negative signal results when the magnetization is stored along the $-z$ axis due to previous pulses. A subsequently applied pulse along the $+x$ axis will then rotate the magnetization onto the $-y$ axis, which corresponds to a negative phase in the spectrum.

At the lowest pressures, the lineshape of the physisorbed xenon peak of the hydrogen terminated and methanol covered samples is asymmetric (Fig. 2). This can be attributed to the ^{129}Xe chemical shift anisotropy or to xenon adsorption in pores of different sizes. Xenon adsorbed in smaller pores gives rise to a higher chemical shift than xenon in larger cavities [20–22]. In the methanol covered sample, the smallest void spaces are likely to be blocked by the methanol and thus inaccessible to the xenon. We expect a damping of the resonance on the downfield side of the peak which is in agreement with the experimental results. By varying dopant type, dopant density and etching conditions in the preparation of porous silicon [15], different regimes of the pore sizes can also be obtained and should help to further develop the present results.

All pore sizes which are accessible to the xenon contribute to the lineshape of the physisorbed xenon resonance. When all pores are equally accessible, this lineshape reflects the pore size distribution. In the hydrogen terminated sample, the lineshape is clearly non-Gaussian. Avnir et al. [23] showed that an adsorption isotherm for a fractal surface can be obtained by replacing the bell-shaped, e.g. Gaussian, distribution in the Dubinin approach [24] for adsorption on structurally heterogeneous microporous materials with the pore size distribution function of a fractal object. With increasing surface irregularity, expressed as fractal dimension D ($D \rightarrow 3$), the number of micropores slightly smaller than the smallest pore size which can be probed by the adsorbate is considerably larger than the number of pores which slightly exceed the upper limit of fractality of the object [23]. The pore size distribution of the hydrogen terminated sample, as characterized by the adsorbate lineshape in the NMR spectrum, agrees well with the pore size distribution of a fractal object.

The lineshape of the adsorbed xenon on the hydrogen terminated sample displayed in Fig. 2 can also be caused by an energetic heterogeneity of the adsorption sites on the surface. The heat of adsorption on a fractally microporous solid increases as the surface geometry becomes more irregular [25]. For a fractal pore size distribution with a large fraction of small pores ($D \rightarrow 3$), the gradual filling of micropores starts with the smallest pores. An energetic heterogeneity would thus result in the observed lineshape of the adsorbed xenon peak on the hydrogen terminated sample.

The ^{129}Xe NMR results for all three samples are summarized in Fig. 3. The chemical shift of the physisorbed xenon resonance is plotted versus the adsorbed volume at standard temperature and pressure. The volumes were calculated according to the BET procedure [26]. The xenon chemical shift is determined by the interaction of the xenon with the surface, characteristic of the material, and by the xenon–xenon interactions. The almost linear dependence of the ^{129}Xe shift on the coverage in the low coverage regime (0.3 cm^3 adsorbed xenon correspond to a coverage of 1.0 ± 0.5 monolayers) indi-

SURFACE SCIENCE LETTERS

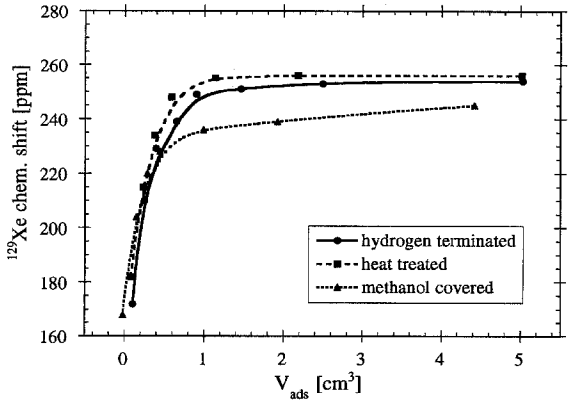

Fig. 3. Dependence of the ^{129}Xe chemical shift for different samples on the adsorbed volume V_{ads} at standard temperature and pressure. V_{ads} also includes xenon which freezes as bulk solid.

cates that only binary collisions of the xenon atoms at or near the surface are important. For a linear dependence, the contribution of the xenon/surface interaction can be obtained by extrapolating the observed shifts to zero xenon pressure, according to the procedure described in Ref. [27]. We obtain an extrapolated chemical shift value δ_{surf} for all three samples of 165 ± 5 ppm. The chemical shift reaches a limiting value δ_{sat} when no more xenon is adsorbed onto the surface and the xenon freezes as bulk solid on the glass walls of the sample tube. This corresponds to the emergence of the signal at 310 ppm in the NMR spectra and a strong increase in the adsorbed volume. For the hydrogen terminated and heat treated samples, δ_{sat} is the same within the experimental error (250–255 ppm). The δ_{sat} value of the methanol covered sample (240 ± 5 ppm) reflects a change in the adsorption properties compared to the other two samples, indicating that the methanol coverage induces a decrease of the adsorption energy for the xenon. Since δ_{surf} is the same for all three samples, the change in δ_{sat} is most likely due to the contribution caused by the xenon–xenon interactions. These interactions are weaker when the total amount of adsorbed xenon diminishes due to a decrease in the adsorption energy.

The increased number of dangling bonds in the heat treated sample is not apparent in the ^{129}Xe chemical shift, but dramatically affects the relaxation behavior of the physisorbed xenon. The interaction of the xenon with the dangling bonds causes a shorter spin lattice relaxation time of the xenon, which is observable in the single scan spectra in a smaller signal to noise ratio under otherwise identical experimental conditions.

To summarize, we have demonstrated the use of physisorbed xenon NMR as a probe of the adsorption properties of porous silicon. The observed lineshapes of the physisorbed xenon resonance at the lowest pressures are non-Gaussian, arising from geometric or energetic heterogeneity of a fractal surface. The observed chemical shift values at the xenon saturation coverage combined with the occurrence of a solid xenon peak reflect the adsorption properties of the porous silicon surfaces. The methanol covered porous silicon displays the lowest adsorption energy for the xenon. It should be noted, that the ^{129}Xe NMR data at the low xenon pressures of 11 to 50 Torr applied in combination with the long ^{129}Xe spin lattice relaxation time (> 10 s) are only accessible by substantial enhancement of the NMR sensitivity through optical pumping.

Acknowledgements

This work was funded by the Director, Office of Energy Research, Office of Basic Energy Sciences, Materials Sciences Division, US Department of Energy, under Contract No. DE-AC03-76SF00098. Thanks to V. Petrova-Koch for supplying the sample. We gratefully acknowledge helpful discussions with V. Petrova-Koch, A.P. Alivisatos and H.C. Gaede.

References

[1] C. Pickering, M.I.J. Beale, D.J. Robbins, P.J. Pearson and R. Greef, J. Phys. C. 17 (1984) 6353.
[2] L.T. Canham, Appl. Phys. Lett. 57 (1990) 1046.
[3] D.S. Chemla and M.B. Miller, J. Opt. Soc. Amer. B 2 (1985) 1155.
[4] D.J. Lockwood, Solid State Commun. 92 (1994) 101.
[5] M. Voos, P. Usan, C. Delalande, G. Bastard and A. Halimaoui, Appl. Phys. Lett. 61 (1992) 1213.
[6] M.B. Robinson, A.C. Dillon, D.R. Haynes and S.M. George, Appl. Phys. Lett. 61 (1992) 1414.

SURFACE SCIENCE LETTERS

[7] S. Banerjee, K.L. Narasimhan, P. Ayyub, A.K. Srivastava and A. Sardesai, Solid State Commun. 84 (1992) 691.
[8] J.M. Lauerhaas, G.M. Credo, J.L. Heinrich and M.J. Sailor, J. Am. Chem. Soc. 114 (1992) 1911.
[9] J.M. Lauerhaas and M.J. Sailor, Science 261 (1993) 1567.
[10] R.C. Anderson, R.S. Muller and C.W. Tobias, J. Electrochem. Soc. 140 (1993) 1393.
[11] T. Ito and J. Fraissard, J. Chem. Phys. 76 (1982) 5225.
[12] D. Raftery and B.F. Chmelka, in: NMR Basic Principles and Progress, Vol. 30, Eds. B. Blümich and R. Kosfeld (Springer, Heidelberg, 1994) p. 111.
[13] (a) A. Kastler, J. Phys. Radium 11 (1950) 255.
(b) N.D. Bhaskar, W. Happer and T. McClelland, Phys. Rev. Lett. 49 (1982) 25.
(c) N.D. Bhaskar, W. Happer, M. Larsson and X. Zeng, Phys. Rev. Lett. 50 (1983) 105.
(d) W. Happer, E. Miron, S. Schaefer, D. Schreiber, W.A. van Wijngaarden and X. Zeng, Phys. Rev. A 29 (1984) 3092.
[14] D. Raftery, H. Long, T. Meersmann, P.J. Grandinetti, L. Reven and A. Pines, Phys. Rev. Lett. 66 (1991) 584.
[15] P.C. Searson, J.M. Macaulay and S.M. Prokes, J. Electrochem. Soc. 139 (1992) 3373.
[16] F. Koch, V. Petrova-Koch and T. Muschik, J. Lumin. 57 (1993) 271.
[17] C.R. Bowers, T. Pietrass, E. Barash, A. Pines, R.K. Grubbs and A.P. Alivisatos, J. Phys. Chem. 98 (1994) 9400.
[18] D. Raftery, H. Long, L. Reven, P. Tang and A. Pines, Chem. Phys. Lett. 191 (1992) 385.
[19] (a) G.R. Davies, T.K. Halstead, R.C. Greenhow and K.J. Packer, Chem. Phys. Lett. 230 (1994) 237.
(b) H.C. Torrey, Phys. Rev. 130 (1963) 2306.
(c) R.L. Streever and H.Y. Carr, Phys. Rev. 121 (1961) 20.
(d) E.R. Hunt and H.Y. Carr, Phys. Rev. 130 (1963) 2302.
[20] J.A. Ripmeester and W. Davidson, J. Mol. Struc. 75 (1981) 67.
[21] J.A. Ripmeester, C.I. Ratcliffe and J.S. Tse, J. Chem. Soc., Faraday Trans. 1 84 (1988) 3731.
[22] T.T.P. Cheung, J. Phys. Chem. 93 (1989) 7549.
[23] D. Avnir and M. Jaroniec, Langmuir 5 (1989) 1431.
[24] M.M. Dubinin, in: Characterization of Porous Solids, Vol. 39, Eds. K.K. Unger, J. Rouquerol, K.S.W. Sing and H. Kral (Elsevier, Amsterdam, 1988) p. 109.
[25] M. Jaroniec, X. Lu, R. Madey and D. Avnir, J. Chem. Phys. 92 (1990) 7589.
[26] S. Brunauer, P.H. Emmett and E. Teller, J. Am. Chem. Soc. 60 (1938) 309.
[27] D. Raftery, L. Reven, H. Long, A. Pines, P. Tang and J.A. Reimer, J. Phys. Chem. 97 (1993) 1649.